

Exsolution in metamorphosed chromite from the Red Lodge district, Montana

PATRICIA J. LOFERSKI AND BRUCE R. LIPIN

U.S. Geological Survey, M.S. 954

Reston, Va 22092

Abstract

Chromite in ultramafic rocks near Red Lodge, Montana has undergone exsolution during upper amphibolite facies metamorphism. Three textural types of exsolved chromites were found. Type A grains consist of an Al-rich host that contains blebs and rare smaller lamellae of an Fe-rich guest. Type A grains are lowest in bulk X_{Cr} ($=Cr/(Cr+Al+Fe^{3+})$), with values less than 0.3. Type B grains have an Fe-rich host that contains blebs and dense networks of lamellae of an Al-rich guest. In Type B, bulk X_{Cr} values are between 0.26 and 0.45. Type C grains contain a very fine intergrowth of Al- and Fe-rich lamellae. Bulk compositions of Type C have $X_{Cr} = 0.47$ to 0.61. All of Type A and many Type B samples show textural evidence of multiple stages of exsolution, such as exsolution within guest phases and abrupt size differences between blebs and lamellae.

On the basis of experimental work and compositional data on the exsolved Red Lodge chromites, a miscibility gap was constructed inside the spinel prism. This miscibility gap is tunnel-shaped and extends from the Fe_3O_4 - $FeAl_2O_4$ - $FeCr_2O_4$ face to the $MgFe_2O_4$ - $MgAl_2O_4$ - $MgCr_2O_4$ face.

If exsolution began at or near the peak temperature of regional metamorphism in the eastern Beartooth Mountains, the temperature of unmixing was near 600°C.

Introduction

The presence of a miscibility gap in the spinel prism, between iron- and aluminum-rich chromite, has been postulated from the occurrence of two coexisting Cr-spinels in some metamorphosed ultramafic rocks (Springer, 1974; Frost, 1975; Berg, 1976; Pinsent and Hirst, 1977). Actual exsolution in chromite is rare, however, and has only been reported in chromite from two locations: the Giant Nickel mine, British Columbia (Muir and Naldrett, 1973) and the Fiskenaeset Complex, Greenland (Ghisler, 1976; Steele *et al.* 1977).

This report describes the textures and compositions of exsolved chromites from metamorphosed ultramafic bodies near Red Lodge, Montana. The exsolution in the Red Lodge chromites is unique because of the variable textures, some of which have not previously been described in chromite. The compositions of the exsolved phases define an extensive miscibility gap in the spinel prism which extends to more chromium-rich compositions than have previously been reported.

Location and general geology

The Red Lodge chromite district is located in the eastern part of the Beartooth Mountains (Fig. 1). Chromite occurs as a ubiquitous accessory mineral and as local segregations in small ultramafic bodies which range from a few tens of meters up to as much as 350 m in maximum dimension. Chromite was discovered in the

district in 1916 and was mined from some of the deposits during the early 1940's. Detailed descriptions of the deposits and production figures are given by James (1946) and Simons *et al.* (1979).

The Beartooth Mountains form a northwest-trending, rectangular block about 65 by 115 km that was uplifted along high-angle reverse faults during the Laramide orogeny. Most of the eastern part of the range consists of Archean granitic gneisses, generally thought to have an igneous origin, migmatites, and pegmatites. The ultramafic rocks form concordant lenses in an interlayered sequence of amphibolite, quartzite, biotite schist, and banded ironstone (Eckelmann and Poldervaart, 1957; Casella, 1969; Simons *et al.*, 1979), which form isolated roof pendants in the granitic gneiss.

The ultramafic rocks and contained chromites were subjected to regional metamorphism to upper amphibolite and locally to granulite facies about 2800 m.y. ago (Eckelmann and Poldervaart, 1957; Gast *et al.*, 1958; Casella, 1969; Skinner, 1969; Simons *et al.* 1979), and to greenschist facies metamorphism about 1600-1800 m.y. ago (Nunes and Tilton, 1971; Rowan and Mueller, 1971; Page, 1977). The ultramafic rocks consist of hornblendites, serpentized dunites, and serpentized peridotites. In the ultramafic rocks, the relict prograde metamorphic minerals are hornblende, orthopyroxene, clinopyroxene, and olivine. Retrograde minerals include serpentine, talc, chlorite, phlogopite, carbonate minerals, and magnetite.

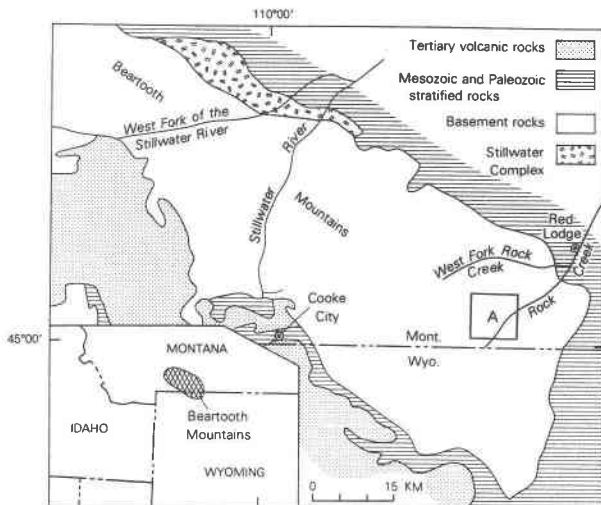


Fig. 1. Geologic map of the eastern Beartooth Mountains showing the location of the study area (A) (modified from Page, 1979).

Retrograde alteration, especially serpentinization, has been extensive in many of the rocks.

The origin of the ultramafic bodies is uncertain. On the basis of field evidence, especially the isolated occurrence and lense-like shapes of the bodies, James (1946) concluded that they were alpine-type. Other evidence, however, indicates strong similarities to stratiform-type deposits. This evidence includes: (1) the fine grain size of chromite (generally less than 1 mm diameter) and the absence of nodules; (2) the high-Fe content of the single phase chromite; (3) the absence of rock-types commonly associated with alpine ultramafic rocks; and (4) the Archean age and the geologic setting. It is believed that the Red Lodge ultramafic bodies were originally parts of a stratiform-type complex that was tectonically disrupted and emplaced as fragments during the regional metamorphism (Loferski, 1980a). The ultramafic rocks in the nearby Highline Trail Lakes area, Wyoming, may also be fragments of a disrupted stratiform intrusion (Skinner, 1969).

Methods

Samples were collected from open-pit chromite mines on Silver Run, Hellroaring, and Line Creek Plateaus. Samples collected by H. L. James in 1942 were also analyzed in the present study. The rocks were studied by standard optical techniques using both transmitted and reflected light. Individual mineral grains were analyzed with an electron microprobe and data were reduced by the method of Bence and Albee (1968). In the microprobe analyses, Fe is reported as total FeO and as calculated Fe_2O_3 and FeO, along with the resulting new totals. Calculation of Fe^{3+} in the mineral formulae was done assuming ideal spinel stoichiometry.

Nomenclature

Nomenclature of spinel-group minerals is ambiguous because of extensive solid solution among many end-members and because end-member names are applied to solid solutions. Traditionally, the name chromite has been used for a wide variety of spinel compositions, the only requirement being that Cr_2O_3 content is greater than about 15 weight percent (Thayer, 1973). We have modified Thayer's definition for the purposes of this paper, and consider any spinel having $X_{\text{Cr}} > 0.15$ as chromite regardless of its $\text{Mg}/(\text{Mg} + \text{Fe}^{2+})$ (see Table 1). Under this system the name magnesiochromite would apply only to pure MgCr_2O_4 . For compositions in which $X_{\text{Cr}} < 0.15$, Al/Fe^{3+} and Mg/Fe^{2+} ratios determine the name.

Some of the exsolved chrome spinels from Red Lodge have $X_{\text{Cr}} < 0.15$, and in this paper, when referred to individually, they are named according to the system in Table 1. However, for convenience, we refer to the entire group of exsolved chrome spinels as the Red Lodge chromites or exsolved chromites, and we include those few that do not meet our definition of chromite.

It should be pointed out that the exsolution discussed here is quite distinct from the typical ferritchromite (Spangenberg, 1943) type of chromite alteration found in many ultramafic rocks. Ferritchromite is an Fe-rich, Mg- and Al-depleted oxide (Table 2), commonly accompanied by chlorite, that forms along chromite rims and cracks in

Table 1. Spinel ($\text{A}^{2+}\text{B}_2^{3+}\text{O}_4$) nomenclature based on divalent and trivalent cations

Endmember names (Deer, Howie, and Zussman, 1966)		
	A^{2+}	B^{3+}
Spinel	Mg	Al
Hercynite	Fe	Al
Magnesioferrite	Mg	Fe
Magnetite	Fe	Fe
Magnesiochromite	Mg	Cr
Chromite	Fe	Cr
Working definitions for this paper		
$*X_{\text{Cr}} > 0.15$	chromite	
$X_{\text{Cr}} < 0.15$ and		
1) $\text{Mg} > \text{Fe}^{2+}$, $\text{Al} > \text{Fe}^{3+}$	spinel	
2) $\text{Fe}^{2+} > \text{Mg}$, $\text{Al} > \text{Fe}^{3+}$	hercynite**	
3) $\text{Mg} > \text{Fe}^{2+}$, $\text{Fe}^{3+} > \text{Al}$	magnesioferrite**	
4) $\text{Fe}^{2+} > \text{Mg}$, $\text{Fe}^{3+} > \text{Al}$	magnetite	
$*X_{\text{Cr}} = \text{Cr}/(\text{Cr} + \text{Al} + \text{Fe}^{3+})$		
**Compositions not encountered in this study.		

Table 2. Ferritchromit analyses from other locations

	1.	2.	3.	4.	5.	6.	7.
Cr ₂ O ₃	56.0	42.0	38.8	37.8	28.10	14.87	13.9
Al ₂ O ₃	1.8	3.1	0.29	0.3	0.26	0.06	1.0
Fe ₂ O ₃	13.1	22.4	30.4	—	39.30	55.05	—
FeO	14.7	30.16	25.2	52.1	27.90	25.97	76.2
MgO	10.1	2.1	3.09	3.3	2.29	3.15	3.0
MnO	0.49	n.d.	0.43	n.d.	0.39	0.47	n.d.
TiO ₂	0.12	1.04	<0.02	n.d.	0.31	0.42	0.6
MnO	0.47	n.d.	0.69	n.d.	0.75	n.d.	0.3
Total	96.78	100.80	98.92	93.5	99.3	99.99	95.0

n.d. = not determined.

1. Onyeagocha, 1974, analysis 2-4A#1.
2. Beeson & Jackson, 1969.
3. Hoffman & Walker, 1978, analysis 6-7-8, p. 705.
4. Ulmer, 1974.
5. Pinsent & Hirst, 1977, analysis 60186(F), p. 589.
6. Bliss & MacLean, 1975, analysis 17, p. 977.
7. Springer, 1974, analysis A41B, p. 177.

lower grade rocks and as homogeneous grains in high-grade metamorphic rocks. Discussions of the occurrence and genesis of ferritchromit are presented elsewhere (Beeson and Jackson, 1969; Onyeagocha, 1974; Springer, 1974; Ulmer, 1974; Bliss and MacLean, 1975; Hoffman and Walker, 1978; Loferski, 1980a).

Compositionally, much of the chromite reported in this study is in the range of what others have called ferritchromit. However, we avoid the term in this paper because ferritchromit compositional limits are not well-defined.

Chromite exsolution textures

Of the 63 thin sections and polished sections studied, 15 contain chromite showing exsolution features. Three textural types of exsolved chromite, designated A, B, and C were found, and they fall into three different compositional ranges with respect to Cr, Al, and Fe³⁺ (see Table 3,

and Loferski, 1980b). Within single thin sections, exsolution of only one of the three types is found. Ragged, late-stage magnetite rims are common regardless of exsolution type.

Type A exsolution consists of a weakly reflective, Al-rich chromite host and a highly reflective, Fe-rich guest (Fig. 2a). The Fe-rich guests are variously rounded, square, hexagonal, and irregularly shaped, and their size ranges from a few micrometers to as much as 100 μm in diameter. The guest phase (hereafter called blebs) commonly shows a variety of sizes within single grains. In some grains, large Fe-rich blebs are concentrated near the rims and finer ones in the cores, whereas in other grains, the guests are more randomly distributed. The Fe-rich blebs themselves have undergone subsequent unmixing and contain Al-rich(?) lamellae, less than 0.5 μm wide (Fig. 2b), that are exsolved along three directions within the blebs. The Al-rich host may have undergone the beginning of a second unmixing because tiny isolated needles that may be lamellae of an Fe-rich(?) phase are scattered throughout the Al-rich host.

The texture of Type A grains clearly indicates at least two stages of unmixing. First, the Fe-rich blebs exsolved from the host. At a later stage (or stages): (1) the fine Al-rich lamellae exsolved from the blebs, and (2) the tiny rod-like lamellae(?) exsolved from the host. Type A grains occur in four samples that contain the assemblage hornblende + orthopyroxene + olivine + serpentine + talc + magnetite, and in one serpentinite. The chromite grains are commonly rimmed and veined by late-stage magnetite (Fig. 2a).

In Type B exsolution, many of the blebs are elongated along crystallographic directions, in contrast to Type A in which the blebs are rounded. Chromite with Type B exsolution occurs in five samples, including two serpentinites and three hornblende-bearing rocks. Of the five

Table 3. Characteristics of the exsolved Red Lodge chromites

Exsolution type	Number of samples	Host	Guest	Bulk Cr/(Cr+Al+Fe ³⁺)	Texture(s) of guest(s)
A	5	Al-rich	Fe-rich	≤0.30	a) Rounded, square, and hexagonal blebs that contain Al-rich lamellae (figs. 2a, 2b). b) Minute rod-like lamellae.
B	4	Fe-rich	Al-rich	0.26-0.45	a) Variably shaped blebs commonly with oriented extensions (figs. 3a, 3c). b) Fine lamellae between the blebs (figs. 3b, 3d).
B	1	Al-rich	Fe-rich	0.35	a) Blebs with oriented extensions.
C	5	Lamellae of both Fe- and Al-rich		0.47-0.61	a) Extremely fine lamellar intergrowth.

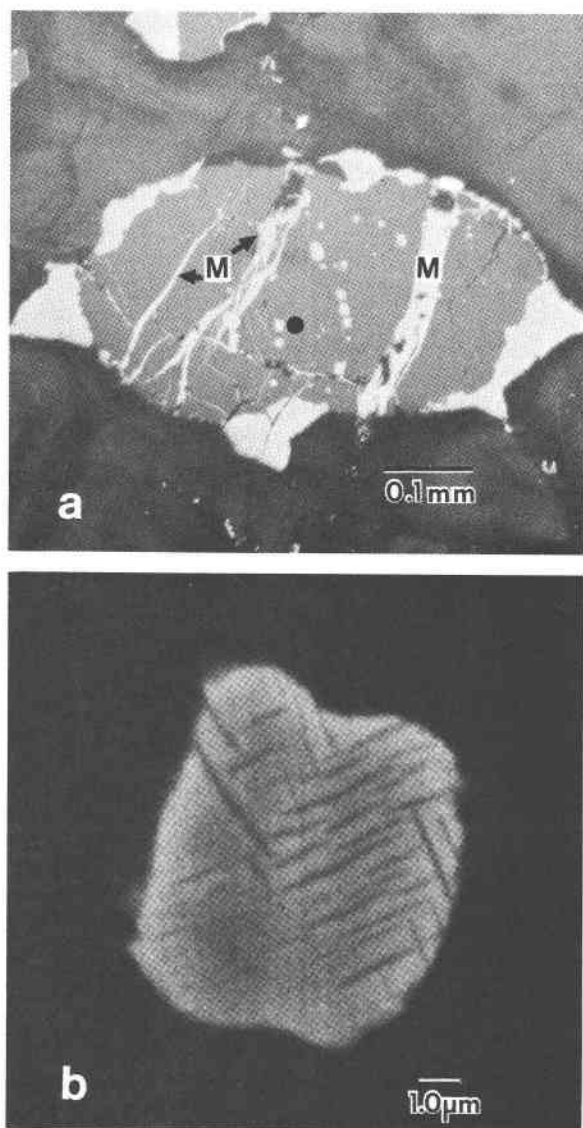


Fig. 2. Photomicrographs of a chromite grain in reflected light from sample HP-20A showing Type A exsolution. (a) Dark-gray Al-rich chromite host with small rounded to rectangular and hexagonal blebs of white Fe-rich guest near the middle, and large irregular masses along the border. The grain is cut by many white magnetite veins (M); the gray silicate matrix is hornblende. (b) A SEM photomicrograph of a bleb, showing fine gray (Al-rich?) lamellae within the bleb. The dot in (a) is adjacent to the bleb shown in (b).

Type B samples, four have a highly reflective Fe-rich host and a weakly reflective Al-rich guest; in the fifth sample, the compositional relationships are reversed (Table 3). Of those samples which have Al-rich guests, the guests have two modes of occurrence. First, they form coarse blebs, commonly 10–20 μm in diameter, and as much as 150 μm in greatest dimension. The shape of the blebs varies from

irregular, to round and sub-rounded, to square and hexagonal forms, and to cruciform and rod-like forms that show sub-parallel orientation along crystallographic directions in the host (see Fig. 3a and 3b near the dot).

Within individual chromite grains, the blebs are variously: (1) randomly scattered throughout grains; (2) concentrated at the grain's rim; or (3) arranged in strings and festoons that have the appearance of defining sub-grain boundaries within the chromite grains. Some of the strings are parallel to the edges of the chromite grains (Fig. 3a).

The second mode of occurrence of the Al-rich guest is as very fine lamellae between the blebs (Fig. 3b). These lamellae have a reflectivity similar to that of the blebs. Like the blebs, the lamellae are Al- and Mg-rich as indicated by X-ray images of a grain for these elements. In Figure 3a, a photomicrograph taken at low magnification, the central area of the chromite grain has a shaded appearance because the fine lamellae are arranged in dense networks. Near some of the coarse blebs, there is a narrow lighter zone that is relatively depleted in lamellae. Optical examination at high magnification reveals that the fine lamellae are intergrown in three directions along {100} of the host (Fig. 3b). Most of the lamellae range from about 0.5 μm down to about 100 \AA , as indicated by transmission electron microscopy. Sub-grain boundaries in chromite grains are defined by the fine lamellae, because their orientation is slightly skewed in adjacent areas within some chromite grains.

Some samples contain grains in which there is an abrupt size discontinuity between the blebs and lamellae (Fig 3b). Other Type B samples contain grains that show a gradation in size between the blebs and the lamellae (Fig. 3c and 3d). In Type B, therefore, some samples show two distinct stages of exsolution in which the coarse blebs exsolved first and were followed by exsolution of the fine lamellae. In other Type B samples, there was a more gradual change from the large blebs to the small lamellae.

Some of the Al-rich blebs in Type B have a mottled texture which suggests that they may be composed of more than one phase (Fig. 3b). A few of the largest blebs do, in fact, contain highly reflective, high-Fe lamellae (Fig. 4). Figure 4 shows three and possibly four different phases: (1) the highly reflective Fe-rich host; (2) the weakly reflective Al-rich bleb; (3) high-Fe lamellae within the bleb, which may or may not be of the same composition as the host; and (4) a phase that rims the bleb and is intermediate in reflectance between the host and guest phases. This fourth "intermediate" phase, which commonly occurs around the Al-rich blebs near the rims and along cracks of Type B chromite grains, is discussed further below.

One of the Type B samples has an Al-rich host and Fe-rich guest, which is the opposite of the other Type B samples. The exsolution in that sample has nevertheless been classified as Type B rather than Type A because of the subparallel elongations of the guest blebs.

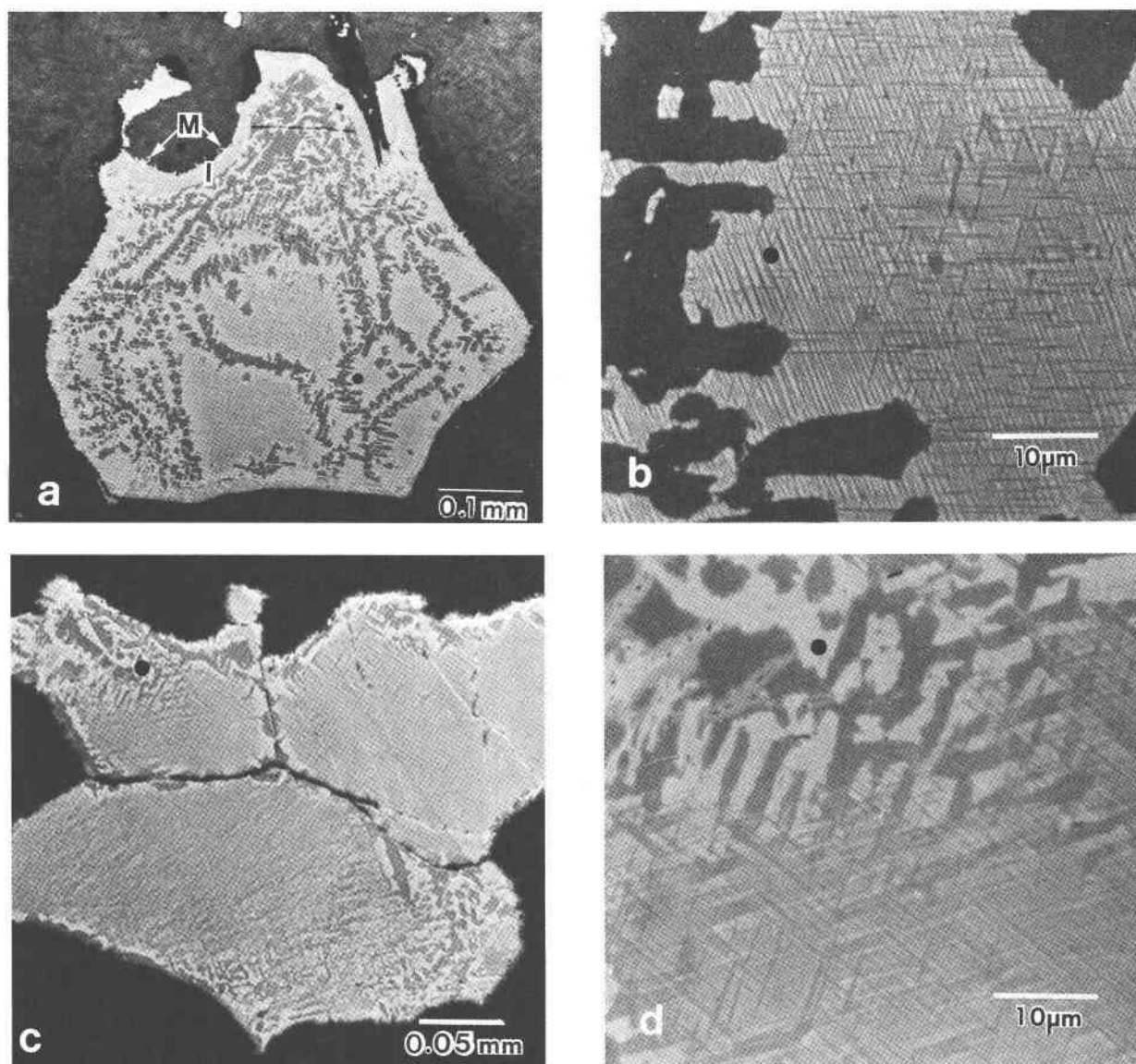


Fig. 3. Photomicrographs of chromite grains in reflected light showing Type B exsolution. (a) From sample SR-2, white Fe-rich chromite host with medium-gray Al-rich blebs, some of which show crystallographic orientation. The blebs form strings in the grain, and some appear to define sub-grain boundaries. The grain has a thin double rim; an inner zone of light-gray Fe-rich chromite (I), and an outer thin zone of lacy magnetite (M). The matrix is serpentine. (b) A close-up of the grain showing fine Al-rich lamellae (gray) between the blebs, intergrown along {100} of the host. Note the abrupt size discontinuity between the blebs and lamellae. The mottled texture in the blebs suggests that they may be composed of more than one phase. (c) A grain from sample HP-14 showing a gradation in size between the blebs and the lamellae. (d) A close-up of the grain in (c), showing the intergradation between coarse and fine intergrowths of Al-rich chromite in Fe-rich chromite. The dots in (a) and (c) correspond to those in (b) and (d), respectively.

Type C exsolution consists of an extremely fine intergrowth of Al-rich chromite lamellae in an Fe-rich chromite host. The intergrowth is just barely visible at magnifications of 1500x and probably continues down to the submicroscopic level. Chromite with Type C exsolution occurs in five samples, including three serpentinites and two hornblende-rich rocks.

Exsolved chromites from the Giant Nickel mine in

British Columbia have various textures (Muir and Naldrett, 1973), some of which appear to be similar to those of Types A and C. The exsolved chromites from the Fiskenaesset Complex, reported by Ghisler (1976) and Steel *et al.* (1977), appear to be similar to Type A exsolution, having a weakly reflective host, and small rounded highly reflective blebs that contain fine, weakly reflective lamellae.

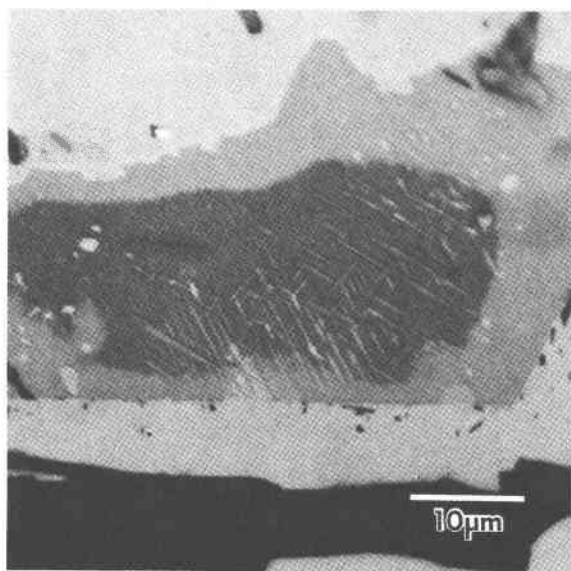


Fig. 4. Photomicrograph in reflected light from sample SR-2 of a large Al-rich bleb (dark-gray) in a Type B grain. The bleb is cut by white (high-Fe?) lamellae and is rimmed by an intermediate medium gray phase.

Compositional relations

The general characteristics of each of the three textural types of exsolution are shown in Table 3. Electron microprobe analyses are given in Table 4 and illustrated in Figures 5 and 6. As noted above, coarse Type A guests and Type B hosts have undergone a second unmixing resulting in extremely fine intergrowths (see Fig. 2b, 3b, and 3d). Type C chromites have undergone only a single unmixing episode, but they too are composed of extremely fine lamellar intergrowths. The lamellae in these samples are too small to analyze separately. Therefore, Type A guest, Type B host, and Type C bulk analyses were carried out using a broad beam in order to obtain the "bulk" composition of these phases.

The compositions of coexisting pairs are plotted on two projections of the spinel prism (Fig. 5). Although there is some overlap, compositional differences between exsolution types exist. The average bulk composition of Type A exsolution is highest in Mg/(Mg+Fe²⁺). Type A also spans the widest compositional gap. Type B and C compositions do not show any appreciable difference in Mg/(Mg+Fe²⁺); however, Type C chromites are generally higher in Cr/(Cr+Al) than even the most Cr-rich Type B guests. Note the general tendency for the slopes of the tie lines to become closer to the vertical as Mg/(Mg+Fe²⁺) decreases (more pronounced in Fig. 5a than 5b). The nearly vertical tie lines are subparallel to and very close to the FeAl₂O₄-FeCr₂O₄-Fe₃O₄ side of the spinel prism.

A plot of the microprobe analyses of the Red Lodge

chromites with respect to Cr-Al-Fe³⁺ is shown in Figure 6. The compositions of Types A, B, and C define a miscibility gap with respect to Cr-Al-Fe³⁺, extending from the Fe³⁺-Al join toward the Cr corner of the diagram. The diagram shows the compositions of the single-phase Red Lodge chromites as well as the exsolved pairs. Most of the single-phase chromites plot closer to the Cr-Al join than to the Cr-Fe³⁺ join; none of them plot within the miscibility gap described by the exsolved spinels.

The three types of exsolved chromite fall in different areas in the miscibility gap. Type A pairs, which have the Al-rich hosts and Fe-rich guests, plot in the region where $X_{Cr} < 0.30$. Type B pairs, which most commonly have the Fe-rich hosts and Al-rich blebs and lamellae, plot in the region where $X_{Cr} = 0.26-0.45$. Type C bulk compositions plot in the region where $X_{Cr} = 0.47-0.61$.

The exsolution textures appear to be controlled by the bulk compositions. Exsolution in Type A compositions results in intergrowths in which the guest forms rounded blebs, a texture in which there is no apparent crystallographic control on the guest shape. There is increased crystallographic control on the guest shape for Type B compositions, as seen in the blebs with elongate extensions along {100}. The Type C exsolved pairs show the greatest degree of shape control, with the very fine lamellar intergrowths.

Of all the exsolved spinels, only two pairs (LC-5 and LC-6) have $X_{Cr} < 0.15$, and are not chromites by our definition (*cf.* Tables 1 and 4). The exsolution in those two pairs of Type A is between Cr-spinel hosts and Cr-magnetite guests. The group of three Type B tie lines that are anomalously short may be the result of the broad electron beam analyses that included the Al-chromite lamellae in the Type B host analyses. A notable feature of the compositions in Figure 6 is that at $X_{Cr} > 0.2$, the tie lines change orientation from being nearly parallel to Fe³⁺-Al to sloping toward Fe³⁺, indicating that Cr partitions preferentially into the Al-chromite rather than the Fe-chromite. On the basis of their study of exsolved chromite from British Columbia, Muir and Naldrett (1973) showed compositions projected onto the Cr-Al-Fe³⁺ plane, but no exsolved chromite had $X_{Cr} > 0.4$. The Red Lodge chromites show a more extensive miscibility gap, to $X_{Cr} = 0.61$.

Experimental work in systems along the faces and edges of the spinel prism has shown that a miscibility gap exists between Fe₃O₄ and FeAl₂O₄ below 860±15°C at 2 kbar (Turnock and Eugster, 1962) and between MgAl₂O₄ and MgFe₂O₄ to above 1300°C at 1 atm (Kwestroo, 1959; Ulmer, 1969). Cremer (1969) reported extensive immiscibility in the FeAl₂O₄-FeCr₂O₄-Fe₃O₄ plane below 900°C at 1 atm and miscibility gaps along the FeAl₂O₄-FeCr₂O₄ and FeCr₂O₄-Fe₃O₄ joins. However, the tie lines predicted by Cremer's experiments do not agree with those shown by natural exsolved spinels (see, for example, Muir and Naldrett, 1973; Steel *et al.*, 1977; and the

Table 4. Microprobe analyses of exsolved chromite

Type A Exsolution										
Sample Location	LC-5 Highline		LC-6 Highline		LC-9 Highline		HP-20A Gallon Jug 1		LC-11 Highline	
	host	guest	host	guest	host	guest	host	guest	host	guest
Cr ₂ O ₃	5.48(.05)*	4.64(.33)	12.11	8.91(.04)	23.63	14.74	21.97(.22)	14.80(1.2)	25.87(.59)	15.77(.03)
Al ₂ O ₃	60.30(.03)	0.52(.13)	51.52	1.99(.22)	35.68	0.44	37.28(.16)	2.36(.45)	35.30(.23)	2.43(.27)
FeO**	17.29(.78)	88.63(.37)	20.06	82.80(.93)	26.98	78.24	30.50(.85)	76.11(.26)	26.79(.73)	74.14(1.5)
MgO	18.06(.33)	0.18(.06)	16.10	0.75(.08)	11.88	1.67	10.59(.001)	0.62(.04)	12.13(.34)	1.85(.29)
NiO	0.41(0.1)	0.50(.01)	0.25	0.54(.01)	0.31	0.55	0.27(.04)	0.63(.08)	0.30(.02)	0.81(.01)
TiO	0.00	0.41(.07)	0.00	0.87(.09)	0.03	0.16	0.06(.01)	1.49(.01)	0.04(.01)	0.28(.01)
Total	101.54	94.88	100.04	95.86	98.51	95.80	100.67	96.01	100.43	95.28
	3***	4	1	3	1	1	3	3	4	2
FeO calc.	14.07	31.02	16.65	31.46	18.89	28.95	21.96	31.97	19.02	28.17
Fe ₂ O ₃ calc.	3.57	64.03	3.79	57.05	9.00	54.78	9.49	49.06	8.63	51.09
New Total	101.89	101.30	100.42	101.57	99.42	101.29	101.62	100.93	101.29	100.40
Formula proportions: cation sum = 3										
Cr	0.111	0.138	0.253	0.259	0.553	0.434	0.506	0.435	0.597	0.462
Al	1.820	0.023	1.666	0.086	1.245	0.019	1.281	0.103	1.214	0.106
Fe ³⁺	0.069	1.815	0.075	1.607	0.199	1.539	0.210	1.379	0.188	1.418
Fe ²⁺	0.302	0.986	0.368	0.967	0.469	0.895	0.534	0.988	0.466	0.881
Mg	0.689	0.010	0.634	0.041	0.525	0.093	0.460	0.034	0.528	0.102
Ni	0.009	0.016	0.004	0.016	0.008	0.016	0.008	0.020	0.006	0.024
Ti	0.000	0.012	0.000	0.024	0.001	0.004	0.001	0.041	0.001	0.007
Cr/R ³⁺	0.06	0.07	0.13	0.13	0.28	0.22	0.25	0.23	0.30	0.23
Fe ³⁺ /R ³⁺	0.03	0.92	0.04	0.82	0.10	0.77	0.11	0.72	0.09	0.71
Cr/(Cr+Al)	0.06	0.86	0.13	0.75	0.31	0.96	0.28	0.81	0.33	0.81
Mg/(Mg+Fe ²⁺)	0.70	0.01	0.63	0.04	0.53	0.09	0.46	0.03	0.53	0.10
Type B Exsolution										
Sample Location	HJ-2a-42 Four Chromes		HP-3 Drill		SR-2 Four Chromes		LC-4 Highline		HP-14 Gallon Jug 2	
	host	guest	host	guest	host	guest	host	guest	host	guest
Cr ₂ O ₃	17.49	31.69	32.30	17.65(.18)	23.29	32.33(.47)	23.62(.69)	33.45(.71)	24.97	34.67
Al ₂ O ₃	2.74	25.16	22.97	2.29(.01)	5.40	18.41(.50)	5.04(.13)	16.80(.62)	4.98	14.98
FeO	71.75	28.31	36.50	74.71(.98)	66.49	45.80(.44)	65.11(1.3)	45.03(.62)	65.11	44.64
MgO	2.25	12.38	7.23	0.85(.07)	0.56	1.75(.32)	1.04(.28)	1.59(.65)	0.71	1.86
NiO	n.d.	n.d.	0.09	0.30(.004)	0.39	0.23(.03)	0.53(.04)	0.29(.03)	0.56	0.36
TiO	0.61	0.16	0.18	0.53(.02)	0.67	0.32(.16)	0.85(.11)	0.58(.07)	0.80	0.60
Total	94.84	97.70	99.27	96.33	96.80	98.84	96.19	97.74	97.13	97.11
	1	1	1	2	1	3	2	6	1	1
FeO calc.	28.70	16.70	24.46	30.63	31.92	32.06	31.25	31.97	31.90	31.25
Fe ₂ O ₃ calc.	47.85	12.90	13.39	48.99	38.43	15.27	37.63	14.51	36.91	14.88
New Total	99.64	98.99	100.62	101.24	100.66	100.37	99.96	99.19	100.83	98.60
Formula proportions: cation sum = 3										
Cr	0.513	0.775	0.814	0.518	0.674	0.865	0.685	0.913	0.721	0.957
Al	0.120	0.918	0.863	0.100	0.233	0.735	0.218	0.683	0.215	0.617
Fe ³⁺	1.333	0.301	0.319	1.354	1.057	0.383	1.050	0.375	1.021	0.394
Fe ²⁺	0.893	0.432	0.655	0.959	0.977	0.913	0.950	0.925	0.967	0.909
Mg	0.124	0.571	0.343	0.047	0.030	0.089	0.057	0.082	0.038	0.097
Ni	n.d.	n.d.	0.002	0.008	0.011	0.006	0.017	0.007	0.016	0.010
Ti	0.017	0.003	0.004	0.014	0.018	0.009	0.023	0.015	0.022	0.016
Cr/R ³⁺	0.26	0.39	0.41	0.26	0.34	0.44	0.35	0.46	0.37	0.49
Fe ³⁺ /R ³⁺	0.68	0.15	0.16	0.69	0.54	0.19	0.54	0.19	0.52	0.20
Cr/(Cr+Al)	0.81	0.46	0.49	0.84	0.74	0.54	0.76	0.57	0.77	0.61
Mg/(Mg+Fe ²⁺)	0.12	0.57	0.34	0.05	0.03	0.09	0.06	0.08	0.04	0.10

present study). Cremer's experiments were synthesis experiments only and should be cautiously interpreted. Experimental information on relationships within the prism at temperatures less than 1000°C is almost non-existent. However, with the experimental data on the edges and faces plus the compositional data from the Red

Lodge chromites, we can begin to construct relationships within the prism. Figure 7 is a sketch of the tunnel-shaped solvus in the spinel prism that extends from the MgAl₂O₄-MgCr₂O₄-MgFe₂O₄ face through the interior of the prism to the FeAl₂O₄-FeCr₂O₄-Fe₃O₄ face. The shape of the miscibility gap on the Fe²⁺ side of the prism

Table 4. (continued)

Sample Location	Type C Exsolution					Intermediate Phase	
	HJ-34a-42 Four Chromes bulk	HJ-1-42 Four Chromes bulk	HP-2 Drill bulk	HP-9 (1) No. Star bulk	HP-9 (2) No. Star bulk	HP-7 Drill bulk	SR-2 Four Chromes bulk
Cr ₂ O ₃	36.09(.66)	40.13(1.7)	38.30(.29)	33.72	42.26	31.41(.72)	30.42(1.0)
Al ₂ O ₃	13.30(.33)	10.23(.33)	4.52(.04)	2.85	2.94	3.74(.36)	0.66(.35)
FeO	41.65(.61)	43.92(1.5)	54.49(.04)	59.71	51.39	60.42(1.1)	65.62(.44)
MgO	6.09(.04)	4.29(.43)	0.14(.01)	0.65	1.72	0.05(.02)	0.34(.08)
NiO	0.20(.4)	n.d.	0.35(.01)	0.23	0.12	0.47(.02)	0.06(.03)
TiO ₂	0.57(.05)	0.36(.06)	0.40(.01)	0.24	0.19	1.04(.45)	0.12(.03)
Total	97.90 3	98.93 3	98.20 2	97.40 1	98.62 1	97.13 3	97.22 3
FeO calc.	24.99	27.67	32.69	31.05	29.81	32.63	31.50
Fe ₂ O ₃ calc.	18.52	18.06	24.22	31.85	23.99	30.89	37.92
New Total	99.76	100.74	100.62	100.59	101.03	100.23	101.02
Formula proportions: cation sum = 3							
Cr	0.966	1.086	1.108	0.984	1.212	0.920	0.899
Al	0.529	0.428	0.195	0.124	0.125	0.163	0.029
Fe ³⁺	0.477	0.469	0.675	0.879	0.653	0.859	1.066
Fe ²⁺	0.702	0.790	0.993	0.964	0.908	1.012	0.983
Mg	0.307	0.218	0.008	0.036	0.093	0.003	0.018
Ni	0.005	n.d.	0.010	0.007	0.004	0.014	0.002
Ti	0.014	0.009	0.011	0.006	0.005	0.029	0.003
Cr/R ³⁺	0.49	0.55	0.56	0.50	0.61	0.47	0.45
Fe ³⁺ /R ³⁺	0.24	0.24	0.34	0.45	0.33	0.44	0.53
Cr/(Cr+Al)	0.65	0.72	0.85	0.89	0.91	0.85	0.97
Mg/(Mg+Fe ²⁺)	0.30	0.22	0.01	0.04	0.09	0.01	0.02

* = standard deviation

**=original microprobe analysis

*** = number of analyses in average

n.d. = not determined

calc. = calculated

is fairly well known because many of the Red Lodge chromite compositions fall near this face (see Fig. 5). No data exist for the Mg-rich side; however, Kwestroo (1959) showed that the miscibility gap along the MgAl₂O₄-MgFe₂O₄ join is skewed toward MgAl₂O₄.

The three tie lines in the miscibility gap (Fig. 7) approximate the compositions of three chromite pairs from Red Lodge. Notice how the tie line for HP-14 is nearly parallel to the FeAl₂O₄-FeCr₂O₄-Fe₃O₄ plane but the tie line for LC-5 extends diagonally from near Fe₃O₄ to near MgAl₂O₄. The direction of the tie lines near the base of the miscibility gap indicates that the assemblage magnetite-spinel is stable with respect to magnesioferite-hercynite at the conditions of exsolution and at low-Cr bulk compositions.

Estimated peak temperatures associated with regional metamorphism in the Red Lodge area range from 500° to 600°C but are closer to 600°C (Eckelmann and Poldervaart, 1957; Prinz, 1964; Casella, 1969; Skinner, 1969), corresponding to the upper amphibolite facies. Skinner presented evidence for local temperature excursions into the granulite facies, perhaps to 700°C, based on the appearance of orthopyroxene in the nearby ultramafic rocks at Highline Trail Lakes. According to Evans (1977),

however, orthopyroxene can appear in the upper amphibolite facies, at 650°C and below.

Olivine-spinel equilibration temperatures, based upon the empirical calibration of Evans and Frost (1975) seem to be in the range of 600-700°C (Fig. 9). The reason for the large uncertainty is the wide range in $Y_{Fe^{3+}}^{Sp}$ (=Fe³⁺/(Cr+Al+Fe³⁺)) in the Red Lodge exsolved chromite. The data of Evans and Frost were based upon chromite with low $Y_{Fe^{3+}}^{Sp}$ (<0.12, normalized to 0.05) and the method does not seem to apply to chromite with $Y_{Fe^{3+}}^{Sp}$ greater than about 0.2. However, those chromite compositions with relatively low $Y_{Fe^{3+}}^{Sp}$ indicate temperatures in the 600-700°C range.

One of the more intriguing aspects of the Red Lodge chromites is the nearly ubiquitous occurrence of the "intermediate" phase in Type A and B samples (Figs. 4 and 8). The composition of the intermediate phase falls outside the miscibility gap (Fig. 6) and yet it exists as a separate phase. The characteristics of this intermediate phase are as follows:

(1) Regardless of exsolution type, the intermediate phase occurs between Al-rich and Fe-rich phases. Texturally, it appears to be the product of reaction between Al-rich and Fe-rich phases.

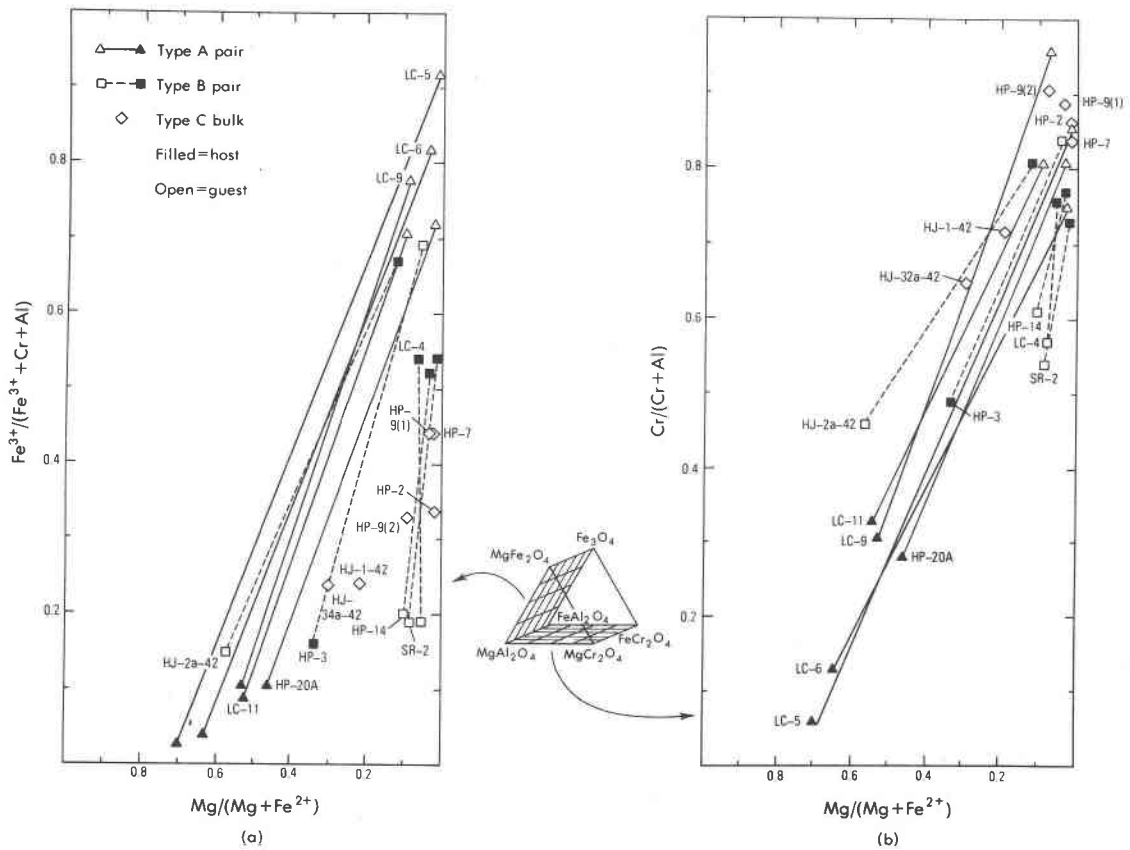


Fig. 5. Compositional plots of exsolved chromites of Types A, B, and C. Type A "guest", Type B "host", except HP-3, and all Type C analyses are combinations of Fe-rich chromite and finely intergrown Al-rich lamellae.

(2) It occurs around some Type A grains at contacts with late magnetite rims.

(3) It forms halos around some guest blebs in both Type A and B grains, near rims and cracks. The halo is thickest on the side of the bleb nearest the rim or crack of the grain in which it occurs.

(4) As rims and cracks are approached, the Al-chromite blebs of Type B disappear leaving only the intermediate phase (Fig. 8).

(5) The intermediate phase has itself undergone unmixing. The lighter lamellae in Figure 4 are indistinguishable from the host phase. In most areas, the unmixing appears to be random and not oriented, and it gives the intermediate phase a mottled texture.

(6) An electron microprobe analysis of a relatively homogeneous looking part of the intermediate phase from Type B reveals that its composition is between Fe_3O_4 and $FeCr_2O_4$ and that it contains almost no Al or Mg (see Table 4 and Fig. 6).

Its occurrence near rims and cracks suggests that the intermediate phase may be the result of Al loss and perhaps some Fe gain toward the outside of the grains. In this aspect the intermediate phase resembles ferritchromite rims.

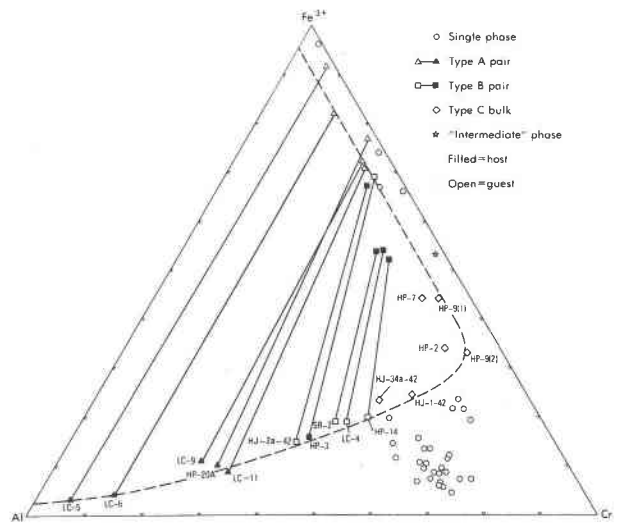


Fig. 6. Compositional plot of exsolved and single-phase Red Lodge chromites. The exsolved pairs define a miscibility gap that extends from the Fe^{3+} -Al join to $Cr/(Cr + Al + Fe^{3+}) = 0.61$. The approximate position of the solvus (dashed line) was drawn by eye.

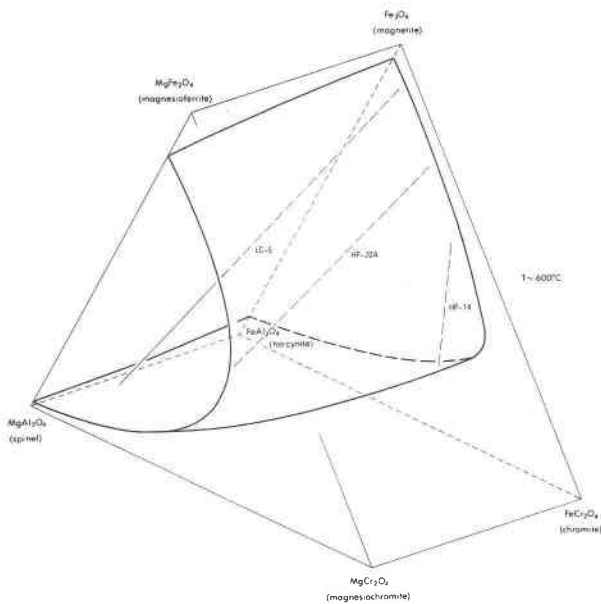


Fig. 7. The conventional view of the spinel prism showing the miscibility gap (heaviest lines) through the prism. Broken lines within the miscibility gap are tie lines from compositions of exsolved chromites from Red Lodge. For further explanation see text.

Simple reaction between Al-chromite and Fe-chromite to form the intermediate phase is unlikely. For two immiscible phases to react to form a single phase under isochemical conditions, there would either have to be a

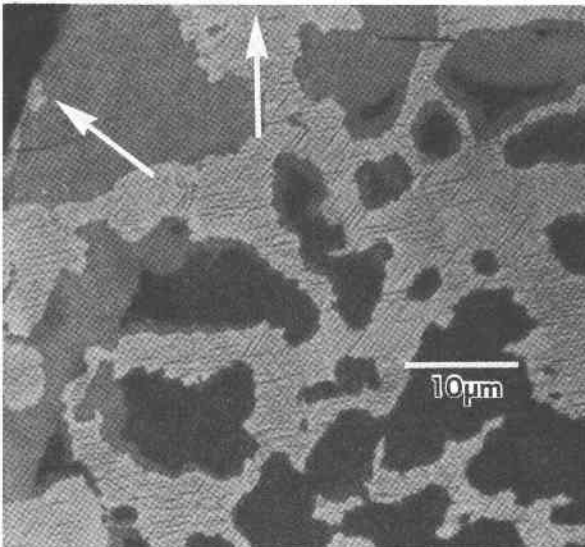


Fig. 8. Photomicrograph in reflected light of the rim of a Type B grain from sample SR-2, showing the "intermediate" (medium gray) phase around Al-rich blebs (dark gray). Note that the "intermediate" phase halos are thickest toward the rim of the grain, and that next to the rim of the grain it appears that the "intermediate" phase has completely replaced the blebs. The arrows point toward the rim of the grain.

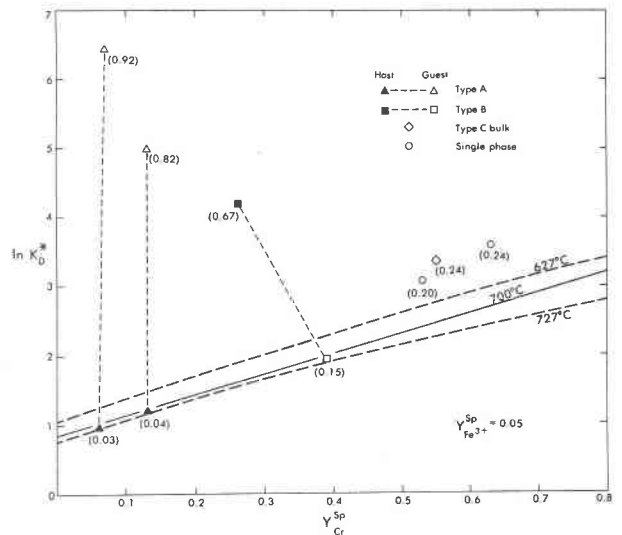


Fig. 9. $\ln K_D$ vs. Y_{Cr}^{Sp} for Red Lodge chromite-olivine pairs. Sp = spinel; Ol = olivine;

$$K_D = \frac{X_{Mg}^{Ol} X_{Fe^{2+}}^{Sp}}{X_{Fe^{2+}}^{Ol} X_{Mg}^{Sp}}; Y_{Cr}^{Sp} = Cr/(Cr+Al+Fe^{3+});$$

$$Y_{Fe^{3+}}^{Sp} = Fe^{3+}/(Fe^{3+}+Cr+Al).$$

Numbers next to the symbols are $Y_{Fe^{3+}}^{Sp}$ of the chromite. The isotherms are for $Y_{Fe^{3+}}^{Sp} = 0.05$. The solid isotherm is from Evans and Frost (1975), dashed isotherms from a thesis by Engi (1978) as reported by Henry and Medaris (1980).

second reheating above the temperature of unmixing or the miscibility gap would have to close at lower temperatures. No evidence exists for either situation. In addition, when two phases react to form a single phase, the composition of the product should be between the reactants. In the Red Lodge chromites, this is not the case (Fig. 6).

One possible explanation for the existence of the intermediate phase is shown in Figure 10, which is a hypothetical three-component system. Although it is usually dangerous to reduce a complex six-component system to three, the Al-chromite guest, the Fe-chromite host, and the intermediate phase in Type B are all very low in Mg and the compositions of all three phases are close to the $FeAl_2O_4$ - $FeCr_2O_4$ - Fe_3O_4 plane, so that geometric distortion is minimized.

At some temperature, T_1 (Fig. 10a), bulk composition x_1 will unmix to form the stable assemblage of q_1+r_1 . Then at some lower temperature, T_2 (Fig. 10b), the miscibility gap intersects the B-C join and the resulting three phase triangle $q_2-r_2-s_2$ represents the compositions of the stable phases. If component A is removed, the bulk composition migrates toward x_2 and new phase s_2 increases at the expense of q_2 while the amount of r_2 stays relatively constant because the path of migration x_1-x_2 is

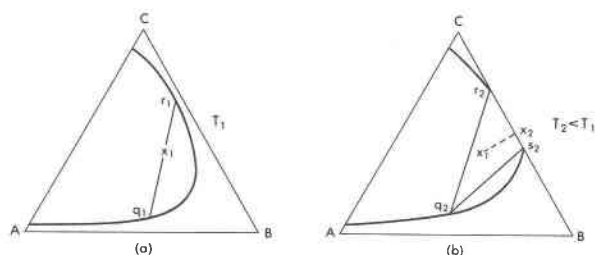


Fig. 10. Expansion of a miscibility gap in a hypothetical system A-B-C so that the gap intersects the B-C join between temperatures T_1 and T_2 . For further explanation see text.

nearly parallel to q_2 - s_2 . Thus, it is possible that the intermediate phase is the result of intersection of the miscibility gap with the $(\text{Mg, Fe})\text{Fe}_2\text{O}_4$ - $(\text{Mg, Fe})\text{Cr}_2\text{O}_4$ face of the spinel prism near the Fe_3O_4 - FeCr_2O_4 join, and the shift in bulk composition causes its occurrence towards rims and cracks.

Scarcity of exsolved chromite

Exsolution of the type we describe here is rare; as we have noted, Red Lodge is only the third locality from which exsolved chromite has been reported. The Red Lodge ultramafic rocks have undergone metamorphism, as have the other localities in which exsolved chromite was found. Accordingly, we originally speculated that metamorphism might be a necessary condition for chromite exsolution. Recently, however, we found exsolved chromite in the lowest cyclic unit of the Stillwater Complex, Montana, in rocks from the Mountain View area. These chromite-bearing, olivine cumulates are partially serpentinized, but they retain their original igneous textures and are not metamorphosed. Evidently metamorphism is not always a necessary condition for chromite exsolution. At Red Lodge, however, at least some of the exsolution was caused by the high-grade metamorphism, because the bulk compositions of some of the exsolved chromite and of the single-phase chromite follow metamorphic rather than igneous trends (Loferski, 1980a).

The exsolved chromite in all four localities is in differentiated gabbroic bodies, and we speculate that this attribute may be necessary for the formation of exsolved chromite. Chromite in differentiated gabbroic bodies tends to be richer in Fe^{3+} than chromite from alpine-type peridotites, and hence the compositions are closer to (or within) the miscibility gap. In addition, the iron enrichment of chromite that accompanies metamorphism or hydrothermal alteration would place the compositions of even more chromite grains inside the miscibility gap. No such exsolution has been reported in chromite from alpine-type peridotites, even those that have undergone regional metamorphism, such as the dunites in the Blue Ridge of North Carolina (Lipin, in prep.).

Evans and Frost (1975, p. 962) show chromite analyses from a contact metamorphosed alpine peridotite in Swit-

zerland that fall within the miscibility gap, but the chromite is not exsolved. The chromite is from a rock composed of olivine + chlorite + enstatite that, according to Evans and Frost, was subjected to 700°C temperatures. Two explanations for this lack of exsolution are possible: (1) the period of time at elevated temperature was too short for unmixing, or (2) inasmuch as the chromite in this body is substantially more magnesium-rich than the Red Lodge chromite, it is possible that the miscibility gap contracts toward the MgCr_2O_4 - MgAl_2O_4 - MgFe_2O_4 face of the prism (Fig. 7). We have drawn the miscibility gap with very little change from one side to the other because of the lack of data on magnesium-rich chromite.

It is possible that exsolved chromite exists in other areas, but has not yet been detected because of the extremely fine-grained nature of some types of exsolution.

Conclusions

(1) The compositions of natural exsolved chromites from Red Lodge, Montana outline a miscibility gap in the Cr-Al- Fe^{3+} plane of the spinel prism. The gap extends from the Fe^{3+} -Al join to much higher Cr contents ($\text{Cr}/(\text{Cr}+\text{Al}+\text{Fe}^{3+}) = 0.61$) than previously reported. When viewed in the spinel prism, the gap is tunnel-shaped and extends from the Fe_3O_4 - FeAl_2O_4 - FeCr_2O_4 face through the prism to the MgFe_2O_4 - MgAl_2O_4 - MgCr_2O_4 face.

(2) For bulk compositions having intermediate Mg contents ($\text{Mg}/(\text{Mg}+\text{Fe}^{2+}) = 0.4$ - 0.6), the assemblage magnetite + spinel is stable with respect to hercynite + magnesioferrite.

(3) The peak metamorphic temperature reached at Red Lodge was about 600°C , which is presumably the temperature at which unmixing of many of the chromites began.

(4) All the reported cases of chromite unmixing are from differentiated gabbroic bodies (Muir and Naldrett, 1973; Ghisler, 1976; Steele *et al.*, 1977; this report) raising the possibility that such a phenomenon is unique to this geological environment.

Acknowledgments

The authors gratefully acknowledge H. P. James for kindly providing some samples from Red Lodge; G. L. Nord, Jr. (USGS) provided TEM work and E. B. Steel (NBS) provided SEM photographs. This manuscript was greatly improved by reviews and discussions with B. R. Frost, G. L. Nord, Jr., M. C. Ross, T. P. Thayer, P. Toulmin III, and G. C. Ulmer. This work is part of a thesis by P. J. Loferski at VPI & SU. Support by J. R. Craig and M. C. Gilbert is greatly appreciated.

References

- Beeson, M. H. and Jackson, E. D. (1969) Chemical composition of altered chromites from the Stillwater complex, Montana. *American Mineralogist*, 54, 1084-1100.

- Bence, A. E. and Albee, A. L. (1968) Empirical correction factors for the electron microanalysis of silicates and oxides. *Journal of Geology*, 76, 382–403.
- Berg, J. H. (1976) Metamorphosed mafic and ultramafic rocks in the contact aureoles of the Nain Complex, Labrador, and the miscibility gap between spinel and magnetite in natural Cr–Al–Fe³⁺–Ti spinels. *Geological Society of America Abstracts with Programs*, 8, 773–774.
- Bliss, N. W. and MacLean, W. H. (1975) The paragenesis of zoned chromite from central Manitoba. *Geochimica et Cosmochimica Acta*, 39, 973–990.
- Butler, J. R. (1969) Origin of the Precambrian granitic gneiss in the Beartooth Mountains, Montana and Wyoming. *Geological Society of America Memoir*, 115, 73–101.
- Casella, C. J. (1969) A review of the Precambrian geology of the eastern Beartooth Mountains, Montana and Wyoming. *Geological Society of America Memoir*, 115, 53–71.
- Cremer, V. (1969) Die Mischkristallbildung im system chromit-magnetit-hercynit zwischen 1000° und 500°C. *Neues Jahrbuch für Mineralogie, Abhandlungen*, 111, 184–205.
- Deer, W. A., Howie, R. A., and Zussman, J. (1966) *An Introduction to the Rock-forming Minerals*. Longman, London.
- Eckelmann, F. D. and Poldervaart, A. (1957) Geologic evolution of the Beartooth Mountains, Montana and Wyoming. Part I. Archean history of the Quad Creek area. *Geological Society of America Bulletin*, 68, 1225–1262.
- Evans, B. W. (1977) Metamorphism of alpine peridotite and serpentinite. *Annual Review of Earth and Planetary Sciences*, 5, 397–447.
- Evans, B. W., and Frost, B. R. (1975) Chrome–spinel in progressive metamorphism—a preliminary analysis. *Geochimica et Cosmochimica Acta*, 39, 959–972.
- Freer, R. (1980) Bibliography Self-diffusion and impurity diffusion in oxides. *Journal of Materials Science*, 15, 803–824.
- Frost, B. R. (1975) Contact metamorphism of serpentinite, chloritic blackwall, and rodingite at Paddy-Go-Easy Pass, Central Cascades, Washington. *Journal of Petrology*, 16, 272–313.
- Gast, P. W., Kulp, J. L., and Long, L. E. (1958) Absolute age of early Precambrian rocks in the Bighorn Basin of Wyoming and Montana, and southeastern Manitoba. *American Geophysical Union Transactions*, 39, 322–334.
- Ghisler, M. (1976) The geology, mineralogy and geochemistry of the preorogenic Archean stratiform chromite deposits at Fiskenaasset, West Greenland. *Monograph Series on Mineral Deposits*, 14.
- Henry, D. J. and Medaris, L. G., Jr. (1980) Application of pyroxene and olivine-spinel geothermometers to spinel peridotites in southwestern Oregon. *American Journal of Science*, 280-A, 211–231.
- Hoffman, M. A. and Walker, D. (1978) Textural and chemical variations of olivine and chrome spinel in the East Dover ultramafic bodies, south-central Vermont. *Geological Society of America Bulletin*, 89, 699–710.
- Irvine, T. N. (1965) Chromian spinel as a petrogenetic indicator, Part I—Theory. *Canadian Journal of Earth Science*, 2, 648–672.
- Jackson, E. D. (1969) Chemical variation in coexisting chromite and olivine in chromitite zones of the Stillwater complex. *Economic Geology Monograph* 4, 41–71.
- James, H. L. (1946) Chromite deposits near Red Lodge, Carbon County, Montana. *U.S. Geological Survey Bulletin* 945-F, 151–189.
- Kwestroo W. (1959) Spinel phase in the system MgO–Fe₂O₃–Al₂O₃. *Journal of Inorganic and Nuclear Chemistry*, 9, 65–70.
- Loferski, P. J. (1980a) Petrology of chromite-bearing metamorphosed ultramafic rocks from the Beartooth Mountains, Montana. M.S. thesis, Virginia Polytechnic Institute and State University, Blacksburg, Virginia.
- Loferski, P. J. (1980b) Unusual exsolution in metamorphosed chromite from the Beartooth Mountains, Montana. *Geological Society of America Abstracts with Programs*, 12, 472.
- Muir, J. E. and Naldrett, A. J. (1973) A natural occurrence of two-phase chromium-bearing spinels. *Canadian Mineralogist*, 11, 930–939.
- Nunes, P. D. and Tilton, G. R. (1971) Uranium–lead ages of minerals from the Stillwater complex and associated rocks, Montana. *Geological Society of America Bulletin*, 82, 2231–2250.
- Onyegocha, A. C. (1974) Alteration of chromite from the Twin Sisters dunite, Washington. *American Mineralogist*, 59, 608–612.
- Page, N. J. (1977) Stillwater complex, Montana: Rock succession, metamorphism, and structure of the complex and adjacent rocks. *U.S. Geological Survey Professional Paper* 999.
- Page, N. J. (1979) Stillwater complex, Montana: Structure, mineralogy, and petrology of the Basal zone with emphasis on the occurrence of sulfides. *U.S. Geological Survey Professional Paper* 1038.
- Pinsent, R. H. and Hirst, D. M. (1977) The metamorphism of the Blue River ultramafic body, Cassiar, British Columbia, Canada. *Journal of Petrology*, 18, 567–594.
- Prinz, M. (1964) Mafic dike swarms of the southern Beartooth Mountains. Part 5. Geologic evolution of the Beartooth Mountains, Montana and Wyoming. *Geological Society of America Bulletin*, 75, 1217–1248.
- Rowan, L. C. and Mueller, P. A. (1971) Relations of folded dikes and Precambrian polyphase deformation, Gardner Lakes area, Beartooth Mountains, Wyoming. *Geological Society of America Bulletin*, 82, 2177–2186.
- Simons, F. S., Armbrustmacher, T. J., van Noy, R. M., Zilka, N. T., Federspiel, F. E., Ridenour, J., and Anderson, L. A. (1979) Mineral resources of the Beartooth primitive area and vicinity, Carbon, Park, Stillwater, and Sweet Grass Counties, Montana, and Park County, Wyoming. *U.S. Geological Survey Bulletin* 1391-F.
- Skinner, W. R. (1969) Geologic evolution of the Beartooth Mountains, Montana and Wyoming. Part 8. Ultramafic rocks in the Highline Trail Lakes area, Wyoming. *Geological Society of America Memoir*, 115, 19–52.
- Spangenberg, K. (1943) Die Chromitlagerstätte von Tampadel am Zobten. *Zeitschrift für praktische geologie*, 5, 13–35.
- Springer, R. K. (1974) Contact metamorphosed ultramafic rocks in the western Sierra Nevada foothills, California. *Journal of Petrology*, 15, 160–195.
- Steele, I. M., Bishop, F. C., Smith, J. V., and Windley, B. F. (1977) The Fiskenaasset complex, West Greenland, Part III: Chemistry of silicate and oxide minerals from oxide-bearing rocks, mostly from Qeqertarsuaq. *Gronlands Geologiske Undersogelse*, 124.
- Thayer, T. P. (1973) Chromium. In D. A. Brobst and W. R. Pratt,

- Eds., United States Mineral Resources. U.S. Geological Survey Professional Paper 820, 111-121.
- Turnock, A. C. and Eugster, H. P. (1962) Fe-Al oxides: phase relationships below 1000°C. *Journal of Petrology*, 3, 533-565.
- Ulmer, G. C. (1969) Experimental investigations of chromite spinels. In H. D. B. Wilson, Ed., *Magmatic Ore Deposits*. Economic Geology Monograph 4, 114-131.
- Ulmer, G. C. (1974) Alteration of chromite during serpentinization in the Pennsylvania-Maryland district. *American Mineralogist*, 59, 1236-1241.

*Manuscript received, January 11, 1982;
accepted for publication, January 22, 1983.*